Murphy – Medmerry

ADS Supplement

APPENDIX 1

Peter Marshall (Historic England)

Modelling the chronology of burnt mound activity at Medmerry

Chronological modelling of the available radiocarbon dates (Stephenson and Krawiec 2019, table 10.1) was undertaken using the program OxCal v4.3 (Bronk Ramsey 2009; Bronk Ramsey and Lee 2013) and the calibration dataset of Reimer et al. (2013). The algorithms used in the models are defined exactly by the brackets and OxCal keywords on the left-hand side of Figure A1.1 (http://c14.arch.ox.ac.uk/). The outputs from the models, the posterior density estimates are shown in black, and the unconstrained calibrated radiocarbon dates are shown in outline. The other distributions correspond to aspects of the model. For example, the distribution '*burnt_mound_4*' (Fig. A1.1) is the posterior density estimate for the last use of burnt mound 4. In the table below (Table A1.1), the Highest Posterior Density intervals of the posterior density estimates are given in italics.

Table A1.1. Key parameters for burnt mound activity at Medmerry

Parameter	***Highest Posterior Density Interval (95% probability)***
Burnt_mound_1	***1430–1290 cal BC***
Burnt_mound_2	***1670–1525 cal BC***
Burnt_mound_4	***1605–1505 cal BC***
Burnt_mound_5	***1560–1425 cal BC***

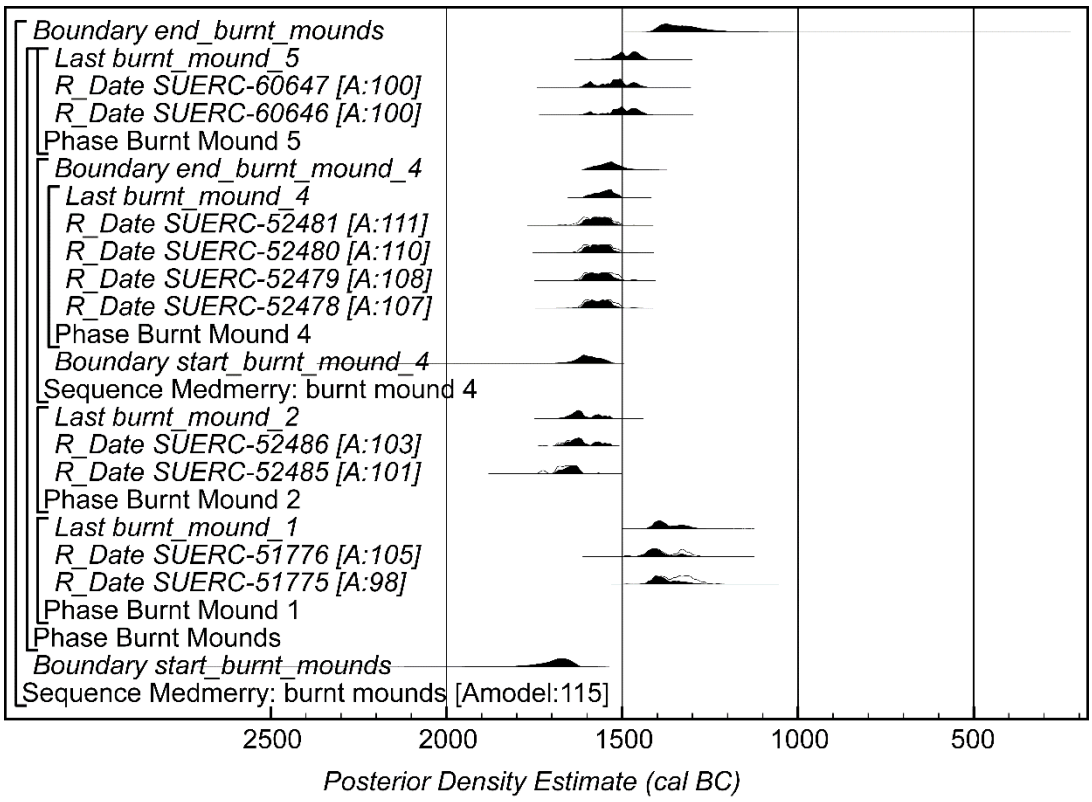

Figure A1.1. Probability distributions for the dates from the Medmerry burnt mounds. Each distribution represents the relative probability that an event occurred at a particular time. For each of the dates two distributions have been plotted, one in outline which is the result produced by the independent calibration of the radiocarbon measurement and a solid one which is based on the chronological information provided by the model. For example, the distribution '*burnt_mound_1*` is the estimated date for the last use of burnt mound 1. The large square brackets down the left-hand side of the diagram, along with the OxCal keywords, define the overall model exactly.

References

Bronk Ramsey, C. 2009. Bayesian analysis of radiocarbon dates. *Radiocarbon*, **51**, 337–360.

Bronk Ramsey, C. and Lee, S. 2013. Recent and planned developments of the program OxCal. *Radiocarbon*, **55**, 720–730.

Reimer, P.J., Bard, E., Bayliss, A., Beck, J.W., Blackwell, P.G., Bronk Ramsey, C., Buck, C.E., Cheng, H., Edwards, R.L., Friedrich, M., Grootes, P.M., Guilderson, T.P., Haflidason, H., Hajdas, I., Hatté, C., Heaton, T.J., Hoffmann, D.L., Hogg, A.G., Hughen, K.A., Kaiser, K.F., Kromer, B., Manning, S.W., Niu, M., Reimer, R.W., Richards, D.A., Scott, E.M., Southon, J.R., Staff, R.A., Turney, C.S..M and van der Plicht, J. 2013. IntCal13 and Marine13 radiocarbon age calibration curves 0–50,000 years cal BP. *Radiocarbon*, **55**, 1869–1887.

Stephenson, P. and Krawiec, K. 2019. *A View from the Edge: Archaeological Investigation on the Manhood Peninsula, Selsey for the Medmerry Managed Realignment.* SpoilHeap Publications Monograph 20. Portslade.

APPENDIX 2

THE HUMAN REMAINS by Dr Paola Ponce (Archaeology South East)

INTRODUCTION

The remains of a skeleton (Police Exhibit No.GJM/1/LA/1) was found on Earnley Beach. The skeleton comprised a cranium (no mandible), eight thoracic vertebrae, a right scapula and a small fragment of bone that probably belongs to the spinous process of a lumbar vertebra. Despite this poor degree of completeness, the bones were in an excellent state of preservation. They were found on a layer of sediment that might have been in recurrent contact with sea water, thus creating an ideal burial environment for bone preservation. The remains were recovered by members of the public, then taken to Sussex Police and later submitted to Cellmark Forensic Services laboratory (Cellmark Ref: CFS/920407/14). The former requested a number of bone fragments to be radiocarbon dated at SUERC Radiocarbon Dating Laboratory in Glasgow University (SUERC Ref: 52367). The results indicated that the bones were of archaeological, not forensic, significance, dating to the Early Iron Age (810-670 cal BC). Following this, the remains of skeleton SK Nº GJM/1/LA/1 were analysed in the Processing Room (Finds Laboratory) at Portslade (Brighton, East Sussex). The initial analysis consisted of preparing an inventory of all bones present, assessing age and sex and diagnosing any evidence of pathological conditions present.

METHOD OF ANALYSIS

Sex estimation

Due to the degree of completeness, the only method used to estimate sex was the observation of dimorphic traits of the skull. This method was applied following the standards proposed by Buikstra and Ubelaker (1994). The features available for observation in SK Nº GJM/1/LA/1 were the supra-orbital ridges, the glabellar profile, mastoid process, posterior zygomatic, and the frontal slope.

Age assessment

It was not possible to assess the age of the skeleton SK Nº GJM/1/LA/1 as all ageing elements such as the ribs, which are necessary for the application of the sternal rib end method (Işcan *et al* 1984) along with the pubic symphysis (Brooks and Suchey 1990) and the auricular surface of the pelvis (Lovejoy *et al* 1985) were absent.

Pathology

The post-excavation analysis included the assessment and diagnosis of basic nature of gross pathology on the skeleton. This analysis was carried out following the diagnostic criteria described in Aufderheide and Rodríguez-Martín (1998) and Ortner (2003).

RESULTS

The assessment of the biological sex suggested that the remains of SK Nº GJM/1/LA/1 were that of a male individual.

As stated above, the age assessment was not possible to be conducted due to the absence of diagnostic skeletal features to carry out this analysis. However, the closure of the sphenoid-basilar suture and the eruption of both maxillary 3rd molars suggested that the individual was 25+ years at the time of death. On the other hand, the ectocranial sutures (coronal, sagittal, lambda), did not show complete obliteration thus rejecting the idea of a senile individual. In other words, there is sufficient evidence to support the hypothesis that the skeleton of SK Nº GJM/1/LA/1 probably belonged to a middle-aged man. This hypothesis was further supported by the presence of osteoarthritis in the spine - a degenerative condition positively correlated with increased age (Jones *et al* 2002; Grotle *et al* 2008), the absence of the upper left third molar, which was lost a long time before death and the upper right, which was intensively worn out.

In terms of pathology, the conditions observed in the skeleton of SK Nº GJM/1/LA/1 were degenerative, trauma, non-specific stress, and dental disease. As mentioned above, the spine was affected by osteoarthritis. Pathognomonic signs of this condition were present in the spine with evidence of *eburnation* (from the Latin *eburnea*, meaning ivory), which results from bone to bone contact/friction and manifests as a polished and sclerotic bone (Bullough 2004). Two thoracic vertebrae (T2 and T9) showed eburnation on their articular facets (the former in the upper right and the latter in the lower left). Another vertebra (T8) did not display signs of eburnation but osteophytes and contour change on the transverse processes, which are also compatible with osteoarthritis.

Trauma was represented by os acromiale on the right scapula, a condition that results from the non-fusion of the acromion of the scapula (Resnick 2002). The ossicle was not present, but the distal end of the acromion exhibited spicules of bone suggesting an attempt of healing and re-union. The glenoid cavity was damaged, and the underlying sub-chondral bone was exposed. It is not known if this resulted from trauma or taphonomic processes. However, the presence of a number of ossified muscles and tendons fibres including the Trapezoid ligament and the *M. Pectoralis Minor* may suggested that these resulted from localised trauma exerted to the shoulder.

Cribra orbitalia, a non-specific stress indicator of poor diet that manifests in sieve-like lesions on the roofs of the orbits, was present on SK Nº GJM/1/LA/1. This was present in a small cluster of porous lesions affecting the right orbit.

Finally, with regards to dental health, the most common pathological conditions present among all maxillary teeth present were dental caries, ante-mortem tooth loss, dental attrition (or dental wear), calculus (mineralised plaque) and periodontal disease.
The maxillary caries present in skeleton SK Nº GJM/1/LA/1 were found on the mesial aspect of the right 1st PM, distal aspect of the left 1st PM and medial aspect of the 2nd PM. Three teeth were lost ante-mortem, the right 1st and 2nd M and the left 3rd M.

Dental attrition was present in all teeth with various degrees of severity. Although this is not considered a pathological condition *per se* (Ortner 2003), excessive dental wear can destroy the enamel of the teeth thus, exposing the dentine to bacterial infection and other dental complications including caries and periodontal disease. Severe dental attrition was observed on the left 1st M whose crown was completely absent, only the root was present. A peri-apical abscess of 1cm in diameter was located just about this tooth exposing part of the root. At first glance the draining cloaca did not seem to be connected to the maxillary sinus but to the root of the adjacent left 2nd M which was absent post-mortem. The other teeth lost post-mortem were the central incisors. Dental calculus was present as fine lines at the cemento-

enamel junction of the right-side maxillary teeth. Dental calculus might have not survived on the left side due to its scarce presence. Lastly, periodontal disease with its various degrees of root exposure severity was observed in all present teeth, thus suggesting the poor oral health of this individual.

DISCUSSION AND CONCLUSION

During the Iron Age, the disposal of the dead included a number of varied funerary practices such as burying the person inside a coffin and within a grave or cist grave, a small barrow surrounded by ditched enclosures and being part of formal cemeteries (Roberts and Cox 2003). During this period there was also a developed interest in wet places (Darvill 1987) and the disposal of bodies in areas or specific ways where they would never be found or retrieved. Bog bodies such as that of Lindow Man found in Cheshire (North West England) is an example of ritual deposition of bodies in water (Connolly 1985). Other Iron Age burial practices included skeletons buried with parts missing, and burials of individual bones, disarticulated joints, excarnation or scattering of cremated remains, or complete inhumations associated with articulated or partially articulated faunal remains (Roberts and Cox 2003; Madgwick 2008). To summarise, many of the burial practices observed during the Iron Age seem to fit with the evidence available for skeleton SK Nº GJM/1/LA/1 (see above).

In terms of disease and in line with the report by Roberts and Cox (2003), osteoarthritis of the spine with evidence of eburnation was a very common disease during the Iron Age period. Spinal joint disease alone accounted for 23% (137/591 individuals recorded). Despite the age-related underlying factor in the onset of osteoarthritis, physical activities related to agricultural tasks such as clearing and ploughing fields, planting and cultivating crops, harvesting and processing crops might have placed a potential health risk to the spine and also to other joints.

Os acromiale has been observed in only one individual (1/252 individuals) reported during the Iron Age period (Roberts and Cox, 2003). Although trauma can be seen as resulting from accident, interpersonal violence or defence, os acromiale within this context may be better understood as related to occupation. For instance, Stirland (2000) presented evidence for an association between os acromiale and archery which will certainly imply an underlying activity-related aetiology of this condition and the possible adscription of a profession or skill to this in individual.

Finally, along with dental disease, cribra orbitalia is another stress indicator commonly found affecting Iron Age populations at a rate of 5.4% (32 people of 591) according to Roberts and Cox (2003).

Dental disease is also a reflection of the subsistence economy maintained during the Iron Age period. According to Roberts and Cox (2003) 7.5% (44/591) studied individuals from this period exhibit some kind of dental disease. For instance, carious lesions have been listed affecting these populations along with the presence of abscesses, periodontal disease, calculus, and ante-mortem tooth loss among others. Intensification in agriculture during this period and the consequent reliance on terrestrial foods as supported by the isotopic analysis carried out by Cook (2014) might have contributed to the poor oral health.

To conclude, the remains of SK Nº GJM/1/LA/1 belonged to a male individual of probable middle age. The diseases and ailments that he suffered seem to be consistent with those seen in other contemporary populations and as expected by an Iron Age individual. On the other hand, little is known about the type of burial he received, how his remains were disposed of as well as other social and biological aspects of his identity.

BIBLIOGRAPHY

Aufderheide, A.C. and Rodríguez-Martín, C. 1998**.** *The Cambridge Encyclopedia of Human Palaeopathology*. Cambridge University Press: Cambridge.

Brooks, S., Suchey, J. 1990. Skeletal determination based on the os pubis: a comparison of the Acsadi-Nemeskeri and Suchey-Brooks methods. *Human Evolution*, 5: 227-238.

Buikstra, J.E. and Ubelaker, DH (eds) 1994. Standards for Data Collection from Human Skeletal Remains. *Arkansas Archaeological Research Series* No. 44. Fayettville: Askansas.

Bullough, P. 2004. *Orthopaedic Pathology*. Mosby: Edinburgh.

Connolly, R. 1985. Lindow Man: Britain's Prehistoric bog body. *Anthropology Today*, 1 (5):15-17.

Darvill, T. 1987. *Prehistoric Britain*. Batsford, London.

Grotle, M., Hagen K., Natvig, B., Dahl, F., Kvien, T. 2008. Obesity and osteoarthritis in knee, hip/or hand: An epidemiological study in the general population with 10 years follow-up. *Musculoskeletal Disorders* 9: 132-136.

Işcan, M., Loth, S., Wright R. 1984. Metamorphosis at the sternal rib end: a new method to estimate age at death in white males. *American Journal of Physical Anthropology*, 65:147-56.

Jones, G., Cooley, H., Stankovish, J. 2002. A cross sectional study of the association between sex, smoking, and other lifestyle factors and osteoarthritis of the hand. *The Journal of Rheumatology*, 29: 1719-1724.

Lovejoy, C., Meindl, R., Pryzbeck, T., Mensforth, R. 1985. Chronological metamorphosis of the auricular surface of the ilium: a new method for the determination of adult skeletal age at death. *American Journal of Physical Anthropology*, 68: 14-28.

Madgwick, R., 2008. Patterns in the modification of animal and human bones in Iron Age Wessex: revisiting the excarnation debate. In Davis, O., Sharples, N. and Waddington, K., eds. *Changing Perspectives on the First Millennium BC: Proceedings of the Iron Age Research Student Seminar 2006.* Oxford: Oxbow, 99-118.

Ortner, D. 2003. *Identification of Pathological Conditions in Human Remains*. Amsterdam: Academic Press.

Resnick, D. 2002. Additional congenital or heritable anomalies and syndromes. Diagnosis of Bone and Joint Disorders. Resnick, D. (Ed) W. B. Saunders: Philadelphia: 4561-4631.

Robert, C., Cox, M. 2003. *Health and Disease in Britain: from prehistory to the present day*. Gloucester: Sutton Publishing.

Stephenson, P. 2014. *Archaeological Excavations at Medmerry Managed Realignment, Selsey, West Sussex. A Post-excavation Assessment and Updated Project Design*. ASE Project No: **4888**. Site Code: **SEL10**. ASE Report No: **2014268**. ASE: Portslade.

Stirland, A. 2000. *Raising the Dead. The Skeleton Crew of King Henry VIII's Great Ship, the Mary Rose*. Chichester, John Wiley & Sons, Ltd.

APPENDIX 3

Medmerry radiocarbon dating and chronological modelling

Peter Marshall (Historic England), Irka Hajdas (ETH, Zurich) and Sanne W.L. Palstra (University of Groningen),

Radiocarbon Dating Methods

A total of 12 radiocarbon measurements were obtained on samples of human bone, and waterlogged wood (Table A3.1 and A3.2). All are conventional radiocarbon ages (Stuiver and Polach, 1977).

Pre-treatment, combustion, graphitisation, and measurement by Accelerator Mass Spectrometry (AMS) of human bone and waterlogged wood samples at the Scottish Universities Environmental Research Centre (SUERC) followed the methods outlined in Dunbar *et al* (2016).

The *14*CHRONO Centre, The Queen's University, Belfast processed a single sample of waterlogged wood using methods outlined in Reimer *et al* (2015). The sample was graphitised using zinc reduction (Slota *et al* 1987) and dated by AMS.

At ETH Zurich, samples of waterlogged wood were pretreated using the acid-base-acid (ABA) protocol outlined in Hajdas (2008) and Němec *et al* (2010). Both samples underwent three different pretreatments as the cellulose extracted (Němec *et al* (2010) was initially so small that the samples had very low carbon yields. Thus, a second cellulose pretreatment was undertaken on a larger initial sample size and finally and an ABA pretreatment just in case the second cellulose yield was again All samples were combusted in an elemental analyser and graphitised using the fully automated system described by Wacker *et al* (2010a). Graphite targets were dated using a 200kV, MICADAS AMS as described by Wacker *et al* (2010b), with data reduction undertaken using BATS Wacker *et al* (2010c).

At the University of Groningen, samples of waterlogged were pretreated using the acid-base-acid (ABA) protocol described in Mook and Streurman (1983). After conversion to CO_2 the samples were reduced with H_2 in the presence of Fe and graphitised (Aerts-Bijma *et al* 1997; 2001) and dated using a 200kV, MICADAS AMS (Wacker *et al* 2010b), with data reduction undertaken using BATS (Wacker *et al* 2010c)

Two groups of replicate measurements are available on samples of waterlogged wood that were divided and separately pretreated at ETH Zurich. In both cases the results are statistically consistent at 95% confidence (Table 3; Ward and Wilson 1978) and a weighted mean has been taken as providing the best estimate for the ages of the samples.

Internal quality assurance procedures and international inter-comparisons (Scott *et al* 2007; 2010) indicate no laboratory offsets and validate the measurement precision quoted.

Chronological modelling

Chronological modelling of the available radiocarbon dates (Table A3.1 and A3.2) was undertaken using the program OxCal v4.3 (Bronk Ramsey 2009; Bronk Ramsey and Lee 2013) and the calibration dataset of Reimer *et al*. (2013). The algorithms used in the models are defined exactly by the brackets and OxCal keywords on the left-hand side of Figure A3.1 (http://c14.arch.ox.ac.uk/). The outputs from the models, the posterior density estimates are shown in black, and the unconstrained calibrated radiocarbon dates are shown in outline. The other distributions correspond to aspects of the model. For example, the distribution '*build_roundwood_fence*'t (Fig. A3.1) is the posterior density estimate for the time when the roundwood fence at Medmerry was constructed. In the text and tables, the Highest Posterior Density intervals of the posterior density estimates are given in italics.

Table A3.1: Medmerry beach skeleton radiocarbon and stable isotope results

Laboratory number	Material & context	$\delta^{13}C$ (‰)	$\delta^{15}N$ (‰)	Radiocarbon Age (BP)	Calibrated date (2σ)
SUERC-52367	Human bone, vertebra, male 25+ years	−20.8±0.2	10.9±0.3	2570±30	810–670 cal BC

Table A3.2: Medmerry radiocarbon results. Replicate measurements have been tested for statistical consistency and combined by taking a weighted mean before calibration as described by Ward and Wilson (1978).

Laboratory number	**Sample and context**	**Radiocarbon age (BP)**	**$\delta^{13}C$ (‰) - IRMS**	**$\delta^{13}C$ (‰) - AMS**	***Highest Posterior Density Interval (95% probability)***
MBW 3					
SUERC-66909	Sample 3: waterlogged *Salix*/*Populus* sp.), a horizontal wattling element from a wooden structure in the intertidal zone	337±29	−27.7±0.2		*cal AD 1480–1645*
MBW 4					
UBA-31689	Sample 4: waterlogged *Alnus glutinosa* (K Stewart), one of the upright timbers from a row in this wooden structure in the intertidal zone	278±28	−27.9±0.22		*cal AD 1495–1605 (67%) or 1615–1665 (28%)*
MBW 15					
SUERC-60639	Waterlogged wood, *Salix/Populus* sp. (K Stewart) from fish basket	364±31	−29.9±0.2		cal AD 1460–1635
Roundwood fence					
GrM-14206	Sample MBE 3B.1: waterlogged wood, *Cytisus/Ulex* (D Challinor), outer 3 rings, from hurdle stake, part of fence driven into earlier deposits.	3232±17	−25.7±0.13		*1605–1580 (9%) or 1560–1445 (86%) cal BC*
GrM-14207	Sample 3B.2: waterlogged wood, *Alnus glutinosa* (D Challinor), outer 3–4 rings, from hurdle stake, part of fence driven into earlier deposits.	3301±15	−25.5±0.13		*1620–1525 cal BC*
ETH-88961.1.1	Sample 3B.3: waterlogged wood, *Alnus glutinosa* (D Challinor), outer 3–rings, from hurdle stake, part of fence driven into earlier deposits. Small cellulose pretreated sample.	3300±30		−32.7	
ETH-88961.2.1	Replicate of ETH-8896.1.1. Cellulose sample.	3275±23		−26.7	

ETH-88961.3.1	Replicate of ETH-8896.1.1. ABA pretreated sample	3283±24		−28.7	
ETH-88961	T'=0.4; T'(5%)=6.0; ν=2	3284±15			*1610–1510 cal BC*
Root system					
ETH-88960.1.1	Sample 3A: waterlogged wood, *Quercus* sp., (D Challinor) outer rings of tree root system. Small cellulose pretreated sample.	3881±24		−25.8	
ETH-88960.2.1	Replicate of ETH-8896.1.1. Cellulose pretreated sample.	3881±23		−23.2	
ETH-88960.3.1	Replicate of ETH-8896.1.1. ABA pretreated sample.	3849±24		−27.3	
ETH-88960	T'=1.2; T'(5%)=6.0; ν=2	3871±24			*2460–2290 cal BC*

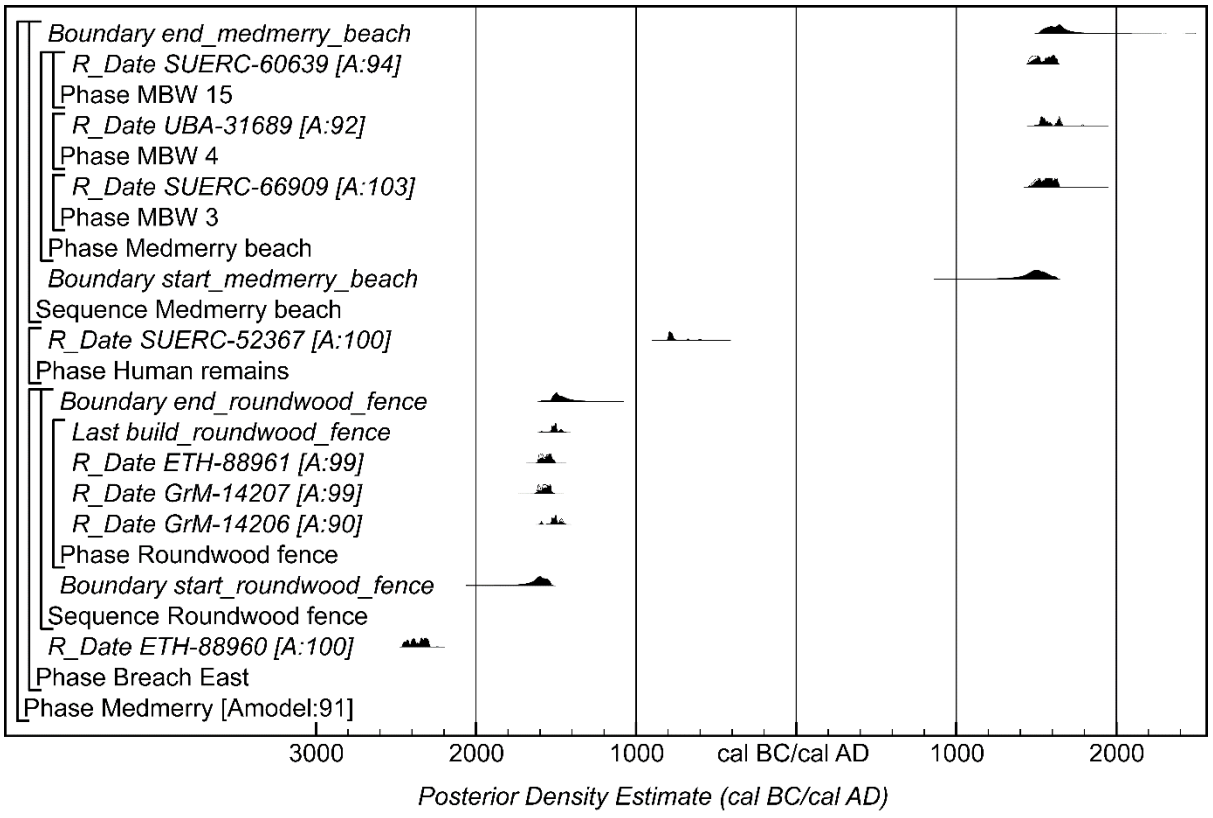

Figure A3.1. Probability distributions for the dates from Medmerry beach. The format is identical to **Figure A1.1**

References

Aerts-Bijma, A.T., Meijer, H.A.J. and van der Plicht, J. 1997. AMS sample handling in Groningen. *Nuclear Instruments and Methods in Physics Research B*, **123**, 221–225.

Aerts-Bijma, A.T., van der Plicht, J. and Meijer, H.A.J. 2001 Automatic AMS sample combustion and CO_2 collection. *Radiocarbon*, **43**, 293–298.

Bronk Ramsey, C. 2009. Bayesian analysis of radiocarbon dates. *Radiocarbon*, **51**, 337–360.

Bronk Ramsey, C. and Lee, S. 2013. Recent and planned developments of the program OxCal. *Radiocarbon*, **55**, 720–730.

Dunbar, E., Cook, G.T., Naysmith, P., Tipney, B.G. and Xu, S. 2016. AMS ^{14}C dating at the Scottish Universities Environmental Research Centre (SUERC) Radiocarbon Dating Laboratory. *Radiocarbon*, **58**, 9–23.

Hajdas, I. 2008. Radiocarbon dating and its applications in Quaternary studies. *Eiszeitalter und Gegenwart Quaternary Science Journal*, **57**, 2–24.

Mook, W.G. and Streurman, H.J. 1983. Physical and chemical aspects of radiocarbon dating. In: Mook, W.G. and Waterbolk, H. T. (eds.) *Proceedings of the First International Symposium ^{14}C and Archaeology*. PACT 8. 31–55.

Reimer, P.J., Bard, E., Bayliss, A., Beck, J.W., Blackwell, P.G., Bronk Ramsey, C., Buck, C.E., Cheng, H., Edwards, R.L., Friedrich, M., Grootes, P.M., Guilderson, T.P., Haflidason, H., Hajdas, I., Hatté, C., Heaton, T.J., Hoffmann, D.L., Hogg, A.G., Hughen, K.A., Kaiser, K.F., Kromer, B., Manning, S.W., Niu, M., Reimer, R.W., Richards, D.A., Scott, E.M., Southon, J.R., Staff, R.A., Turney, C.S..M and van der Plicht, J. 2013. IntCal13 and Marine13 radiocarbon age calibration curves 0–50,000 years cal BP. *Radiocarbon*, **55**, 1869–1887.

Reimer, P.J., Hoper, S., McDonald, J., Reimer, R., Svyatko, S. and Thompson, M. 2015. *The Queen's University, Belfast: Laboratory Protocols used for AMS Radiocarbon Dating at the ^{14}CHRONO Centre*, Portsmouth, English Heritage Research Report **1-2015**.

Scott, E.M., Cook, G.T. and Naysmith, P. 2010. A report on phase 2 of the Fifth International Radiocarbon Intercomparison (VIRI)'. *Radiocarbon*, **52**, 846–858.

Scott, E.M., Cook, G.T., Naysmith, P., Bryant, C. and O'Donnell, D. 2007. A report on Phase 1 of the 5th International Radiocarbon Intercomparison (VIRI). *Radiocarbon*, **49,** 409–426.

Slota Jr., P.J., Jull, A.J.T., Linick, T.W. and Toolin, L.J. 1987. Preparation of small samples for ^{14}C accelerator targets by catalytic reduction of CO. *Radiocarbon*, **29**, 303–306.

Stuiver, M. & Polach, H.A. 1977. Reporting of ^{14}C data. *Radiocarbon*, **19**, 355–363.

Wacker, L., Bonani, G., Friedrich, M., Hajdas, I., Kromer, B., Němec, M., Ruff, M., Suter, M., Synal, H.A. and Vockenhuber, C. 2010. MICADAS: Routine and High-Precision Radiocarbon Dating. *Radiocarbon*, 52, 252–262.

Wacker, L., Christl, M. and Synal, H.A. 2010. Bats: A new tool for AMS data reduction. *Nuclear Instruments and Methods in Physics Research Section B: Beam Interactions with Materials and Atoms*, *268*, 976–979.

Wacker, L., Němec, M. and Bourquin, J. 2010. A revolutionary graphitisation system: Fully automated, compact and simple. *Nuclear Instruments and Methods in Physics Research Section B: Beam Interactions with Materials and Atoms*, **268**, 931–934.

Ward, G.K. and Wilson, S.R. 1978. Procedures for comparing and combining radiocarbon age determinations: a critique. *Archaeometry*, **20**, 19–32.